

Control-Oriented Modeling and Identification of Delta Wing Vortex-Coupled Roll Dynamics

M. Pakmehr, B. W. Gordon and C. A. Rabbath

Abstract—This paper presents the derivation of a control-oriented vortex-based nonlinear state space representation of free-to-roll motion of a delta wing based on a modified nonlinear indicial response method, in conjunction with an internal state-space representation. The relationship among the vortex breakdown location, rolling moment coefficient and roll angle are developed. The proposed model, in fact, integrates the vortex breakdown location on the delta wing surface into the delta wing roll dynamics for control purposes. Different parameter identification methods have been applied to approximate the uncertainties of the nonlinear dynamic model, such as rolling moment coefficient. Experimental results validate the proposed model.

I. INTRODUCTION

A non-linear indicial response (NIR) method, in conjunction with internal state-space (ISS) representation (NIRISS) has been used by X. Z. Huang to describe the vortex breakdown location over a delta wing [1], [2]. It has been found that for a delta wing, its leading edge primary vortex behavior has a dominant effect on its air loads [1], [2]. Consequently, the related air loads applied to the surface of the delta wing and the delta wing attitude can be calculated in terms of the primary vortex breakdown location. In [1], [2], a mathematical model for the case of free-to-roll motion has been presented.

In order to reach the desired roll angle in a given time and improve the efficiency and other dynamic behavior, control algorithms must be designed. As the start up for control algorithms design, the objective of this paper is to develop the state space model for designing control algorithms to be applied to roll dynamics of the delta wing. The proposed model, in fact, integrates the vortex breakdown location on the delta wing surface into the delta wing roll dynamics for control purposes. In order to implement the controllers

more efficiently, different methods have been applied to approximate the uncertain parameters of the system.

Several methods can be found in the literature for the simulation and modelling of vortex breakdown over delta wing and high performance aircraft dynamics and also vortical flows. These methods include computational, neural-network and mathematical methods. Several methods can also be found for the modeling of nonlinear flight dynamics and system identification of nonlinear systems.

In [3], a parabolic distribution for the chord wise axial circulation distribution over slender delta wing has been proposed. Leading-edge vortex breakdown locations have been predicted on the basis of a critical value of the circulation. In [4], a method has been proposed to predict the normal force coefficient acting on a delta wing under static or dynamic conditions.

One of the methods which have been highly used for modelling the uncertain aerodynamics and nonlinear flight dynamics of high performance aircraft and delta wings is nonlinear indicial response (NIR) method initiated by Tobak and his colleagues [16]. This approach represents aerodynamic responses, such as force, moment, etc., due to an arbitrary motion input as a summation of nonlinear responses to a series of “step” motions leading up to step onset.

In [5]-[12], the nonlinear indicial response (NIR) method has been applied for modelling the uncertain aerodynamics and nonlinear flight dynamics in different situations. In [13], the state-space representation of aerodynamic forces and moments for unsteady aircraft motion has been proposed. In [14], the state-space representation of an aerodynamic vortex lattice model has been considered from a classical and system identification perspective. In [15], a short theoretical study of aircraft aerodynamic model equations with unsteady effects has been presented. The aerodynamic forces and moments have been expressed in terms of indicial functions or internal state variables. In [16], basic concepts involved in the mathematical modeling of the aerodynamic response of an aircraft to arbitrary maneuvers have been reviewed. The original formulation of an aerodynamic response in terms of nonlinear functionals has been shown to be compatible with a derivation based on the use of nonlinear functional

Manuscript received September 15, 2004. This work was supported in part by Defence Research and Development Canada (DRDC).

M. Pakmehr and B. W. Gordon are with Department of Mechanical and Industrial Engineering, Concordia University, 1455 de Maisonneuve Blvd. West, Montreal, Quebec, H3G 1M8, CANADA (phone: (514) 848-2424 ext. 8750; fax: (514) 848-3175; e-mail: m_pakmeh@alcor.concordia.ca, bwgordon@me.concordia.ca).

C. A. Rabbath is with Defense R&D Canada – Valcartier, 2459 Pie-XI Blvd North, Val-Belair, QC, G3J 1X5, Canada (e-mail: Camille-Alain.Rabbath@drdc-rddc.gc.ca).

expansions. In [17], the mathematical modeling of the aerodynamic response of an aircraft to arbitrary maneuvers has been reviewed. Bryan's original formulation, linear aerodynamic indicial functions, and superposition have been considered. Ref. [18] is a review of aerodynamic mathematical modeling for aircraft motions at high angles of attack. The mathematical model serves to define a set of characteristic motions from whose known aerodynamic responses the aerodynamic response to an arbitrary high angle-of-attack flight maneuver can be predicted.

In all of the aforementioned research works, the proposed modeling approaches do not result in a model which can be directly implemented for nonlinear control purposes. In this paper, a new dynamic model of a 65° delta wing is proposed. The proposed model relies on the NIRISS method and represents a control-oriented vortex-based nonlinear state space form of free-to-roll motion of a delta wing. The relationship among the vortex breakdown location, rolling moment coefficient and roll angle are developed. The model, in fact, integrates the vortex breakdown location on the delta wing surface into the delta wing roll dynamics for control synthesis. Different parameter identification methods are applied to approximate the uncertainties of the nonlinear dynamic model, such as rolling moment coefficient. Experimental results are utilized to verify the model.

II. STATE SPACE FORMULATION OF SYSTEM WITH NO INPUT

A. Derivation of State Space Formulation

For control synthesis, an appropriate model of the flow over the delta wing is required. The procedure of developing the state space formulation of the nonlinear plant is illustrated in Fig. 1.

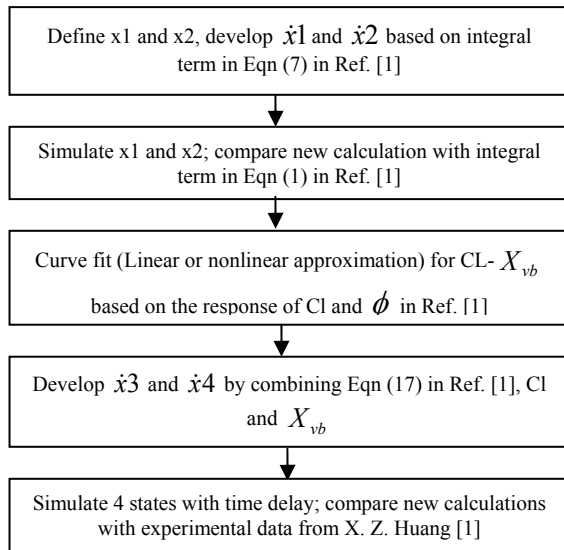


Fig. 1: Procedure of developing the state space formulation.

Vortex breakdown location of free-to-roll motion over a

delta wing is given as [1]:

$$X_{vb} = X_s(\phi(t)) + X_q(\dot{\phi}(t)) \cdot X_s(\phi(t)) + \int_{-T}^t X_u(t-\tau) \dot{\phi}(\tau) d\tau \quad (1)$$

Where the first term represents the static value at time t , and the second and third terms reflect the quasi-steady and unsteady effects.

Two vortices, the left and the right vortex, over the delta wing need to be considered, thus, two vortex breakdown locations, X_{vbl} and X_{vbr} are to be calculated as:

$$X_{vbl} = X_{sl}(\phi(t)) + X_q(\dot{\phi}(t)) \cdot X_{sl}(\phi(t)) + \int_{-T}^t X_{ul}(t-\tau) \dot{\phi}(\tau) d\tau \quad (2)$$

$$X_{vbr} = X_{sr}(\phi(t)) + X_q(\dot{\phi}(t)) \cdot X_{sr}(\phi(t)) - \int_{-T}^t X_{ur}(t-\tau) \dot{\phi}(\tau) d\tau \quad (3)$$

The difference between X_{vbl} and X_{vbr} are the static terms X_{sl} and X_{sr} . The dynamic terms have the same formulation, but the opposite sign.

The static term X_s is assumed by X. Z. Huang to be in parabolic form [1], [2]:

$$\Gamma = C_0 + BX - AX^2 \quad (4)$$

X. Z. Huang considered the dependence of Γ on Leading Edge sweep angle and defined A and B parameters [1]; using his formulation A and B for the left and right vortices are as follows:

$$Al = 1.1 \sin(\alpha) \cdot \sin(\Lambda_l), \quad Bl = 4 \cdot Al \quad (5)$$

$$Ar = 1.1 \sin(\alpha) \cdot \sin(\Lambda_r), \quad Br = 4 \cdot Ar \quad (6)$$

Where effective sweep back angle:

$$\Lambda_l = \lambda_0 - \text{atan}(\tan(\sigma) \cdot \sin(\phi)) \quad (7)$$

$$\Lambda_r = \lambda_0 + \text{atan}(\tan(\sigma) \cdot \sin(\phi)) \quad (8)$$

Where λ_0 and σ are half apex angle and structure angle.

Critical circulation:

$$\Gamma_{cl} = 0.8 \cdot \cos[4 \times (\Lambda_l - \Lambda_e)] \quad (9)$$

$$\Gamma_{cr} = 0.8 \cdot \cos[4 \times (\Lambda_r - \Lambda_e)] \quad (10)$$

Where, Λ_e is obtained by experiments.

The non-dimensional circulation at trailing edge (non-dimensional chord $X=1$) is used to determine the distributions of circulation in chord wise in parabolic form [1].

$$\Gamma l = 5.11 \cdot \left(\Lambda_l + \frac{2.65}{57.3}\right) \cdot \left(\alpha - \frac{3.5}{57.3}\right) \quad (11)$$

$$C_{0l} = \Gamma l - Bl + Al \quad (12)$$

$$\Gamma r = 5.11 \cdot \left(\Lambda_r + \frac{2.65}{57.3}\right) \cdot \left(\alpha - \frac{3.5}{57.3}\right) \quad (13)$$

$$C_{0r} = \Gamma r - Br + Ar \quad (14)$$

The solution of static term X_s is determined as follows [1], which is one possible method of determining X_s .

If $(Bl)^2 + 4 \cdot Al \cdot C_{0l} - 4 \cdot Al \cdot \Gamma_{cl}$ is greater than or equal to 0, then:

$$X_{sl} = \frac{Bl - \sqrt{(Bl)^2 + 4 \cdot Al \cdot C_{0l} - 4 \cdot Al \cdot \Gamma_{cl}}}{2 \cdot Al} \quad (15)$$

Otherwise:

$$X_{sl} = \frac{Bl + \sqrt{(Bl)^2 + 4 \cdot Ar \cdot C_0l - 4 \cdot Ar \cdot \Gamma ct}}{2 \cdot Ar} \quad (16)$$

If $(Br)^2 + 4 \cdot Ar \cdot C_0r - 4 \cdot Ar \cdot \Gamma cr$ is greater than or equal to 0, then:

$$X_{sr} = \frac{Br - \sqrt{(Br)^2 + 4 \cdot Ar \cdot C_0r - 4 \cdot Ar \cdot \Gamma cr}}{2 \cdot Ar} \quad (17)$$

Otherwise:

$$X_{sr} = \frac{Br + \sqrt{(Br)^2 + 4 \cdot Ar \cdot C_0r - 4 \cdot Ar \cdot \Gamma cr}}{2 \cdot Ar} \quad (18)$$

In order to develop the *state equations*, let us first consider the integral term, which is the dynamic term in the model of vortex breakdown location (Eqn 1). Let

$$In = \int_{-T}^t X_u(t-\tau) \dot{\phi}(\tau) d\tau \quad (19)$$

$$a(t) = 1.65 / \tan(\alpha(t)) \quad (20)$$

$$c = \pi / T^* \quad (21)$$

Where $X_u(t-\tau)$ can be obtained from Eqn (12) in [1]:

$$X_u(t-\tau) = \frac{1.65}{\tan \alpha(t)} \sin\left(\frac{\pi(t-\tau)}{T^*}\right) \quad (22)$$

So Eqn (22) is simplified as follows:

$$X_u(t-\tau) = a(t) \cdot \sin(c \cdot (t-\tau)) \quad (23)$$

Expanding Eqn (23), Eqn (24) is obtained:

$$X_u(t-\tau) = a(t) \cdot \sin(ct) \cdot \cos(c\tau) - a(t) \cdot \cos(ct) \cdot \sin(c\tau) \quad (24)$$

Substitute Eqn (24) for $X_u(t-\tau)$ in Eqn (19), the integral term can then be represented as

$$In = a(t) \cdot \sin(ct) \cdot \underbrace{\int_{-T}^t \cos(c\tau) \dot{\phi}(\tau) d\tau}_{z1} - a(t) \cdot \cos(ct) \cdot \underbrace{\int_{-T}^t \sin(c\tau) \dot{\phi}(\tau) d\tau}_{z2} \quad (25)$$

That is

$$In = a(t)(\sin(ct) \cdot z1 - \cos(ct) \cdot z2) \quad (26)$$

In Eqn (26), let

$$x1 = \sin(ct) \cdot z1 - \cos(ct) \cdot z2 \quad (27)$$

Then differentiate $x1$ by t , we have

$$\dot{x1} = \sin(ct) \cdot \dot{z1} - \cos(ct) \cdot \dot{z2} + c(\underbrace{\cos(ct) \cdot z1 + \sin(ct) \cdot z2}_{x2}) \quad (28)$$

In Eqn (28), let

$$x2 = \cos(ct) \cdot z1 + \sin(ct) \cdot z2 \quad (29)$$

Combine Eqn (27) and Eqn (29)

$$\begin{cases} x1(t) = \sin(ct) \cdot z1 - \cos(ct) \cdot z2 \\ x2(t) = \cos(ct) \cdot z1 + \sin(ct) \cdot z2 \end{cases} \quad (30)$$

Rewrite it in matrix form

$$(x) = A(z) \quad (31)$$

$$(z) = A^{-1}(x) \quad (32)$$

Where

$$A = \begin{pmatrix} \sin(ct) & -\cos(ct) \\ \cos(ct) & \sin(ct) \end{pmatrix} \quad (33)$$

$$\det(A) = 1 \quad (34)$$

$$A^{-1} = \begin{pmatrix} \sin(ct) & \cos(ct) \\ -\cos(ct) & \sin(ct) \end{pmatrix} \quad (35)$$

The following integration formula will be used. Let:

$$y(t) = \int_0^t f(\tau) d\tau \quad (36)$$

Then

$$\frac{dy}{dt} = f(t) \quad (37)$$

So for the function

$$y(t) = \int_{-T}^t f(\tau) d\tau \quad (38)$$

Its derivative is

$$\frac{dy}{dt} = f(t) - f(t-T) \quad (39)$$

Based on the above integration formula, differentiate $\mathbf{z1}$ and $\mathbf{z2}$ in Eqn (32) by t respectively

$$\begin{cases} \dot{z1} = \cos(ct) \cdot \dot{\phi}(t) - \cos(c(t-T)) \cdot \dot{\phi}(t-T) \\ \dot{z2} = \sin(ct) \cdot \dot{\phi}(t) - \sin(c(t-T)) \cdot \dot{\phi}(t-T) \end{cases} \quad (40)$$

Let

$$x4(t) = \dot{\phi}(t) \quad (41)$$

Then

$$\begin{pmatrix} \dot{z1} \\ \dot{z2} \end{pmatrix} = \underbrace{\begin{pmatrix} \cos(ct) & -\cos(c(t-T)) \\ \sin(ct) & -\sin(c(t-T)) \end{pmatrix}}_E \underbrace{\begin{pmatrix} x4(t) \\ x4(t-T) \end{pmatrix}}_F \quad (42)$$

That is

$$(\dot{z}) = EF \quad (43)$$

Differentiate $\mathbf{x1}$ and $\mathbf{x2}$ in Eqn (31) by t respectively

$$\begin{pmatrix} \dot{x1} \\ \dot{x2} \end{pmatrix} = \underbrace{\begin{pmatrix} c \cdot \cos(ct) & c \cdot \sin(ct) \\ -c \cdot \sin(ct) & c \cdot \cos(ct) \end{pmatrix}}_C \begin{pmatrix} z1 \\ z2 \end{pmatrix} + \underbrace{\begin{pmatrix} \sin(ct) & -\cos(ct) \\ \cos(ct) & \sin(ct) \end{pmatrix}}_D \begin{pmatrix} \dot{z1} \\ \dot{z2} \end{pmatrix} \quad (44)$$

Substitute Eqn (32) and Eqn (43) for (z) and (\dot{z}) in Eqn (44) results in:

$$(\dot{x}) = CA^{-1}(x) + DEF \quad (45)$$

That is

$$\begin{cases} \dot{x1} = [\cos(ct) \sin(c(t-T)) - \sin(ct) \cos(c(t-T))] \\ \quad \quad \quad x4(t-T) + cx2(t) \\ \dot{x2} = [-\cos(ct) \cos(c(t-T)) - \sin(ct) \sin(c(t-T))] \\ \quad \quad \quad x4(t-T) - cx1(t) + x4(t) \end{cases} \quad (46)$$

Simplifying Eqn (46) and rewrite it, results in Eqn (47):

$$\begin{cases} \dot{x1}(t) = cx2(t) \\ \dot{x2}(t) = -cx1(t) + x4(t) + x4(t-T) \end{cases} \quad (47)$$

The free-to-roll system equation of motion in [1] by defining the *bearing friction* as follows:

$$f_c \cdot \text{sign}(\dot{\phi}) = (b\dot{\phi} / 2u_\infty) \cdot \text{sign}(\dot{\phi}) \quad (48)$$

is written in the following form:

$$I\ddot{\phi} + f_c \cdot \text{sign}(\dot{\phi}(t)) + Cl.q.s.b = 0 \quad (49)$$

For the proposed model Eqn (49) is manipulated to be in the following form:

$$I\ddot{\phi} + f_c \cdot \text{sign}(\dot{\phi}(t)) + Cl.q.s.b = U(t) \quad (50)$$

Where U(t) is input torque in the delta wing roll dynamics. Using Eqn (50) we assume:

$$x_3(t) = \phi(t) \quad (51)$$

$$x_4(t) = \dot{\phi}(t) \quad (52)$$

B. Summaries of State Space formulation

1) Definitions of State Variables

The integral term in X_{vb} equation

$$x_1(t) = \sin(ct)z_1(t) - \cos(ct)z_2(t)$$

A portion in the equation of \dot{x}

$$x_2(t) = \cos(ct)z_1(t) + \sin(ct)z_2(t)$$

Roll angle

$$x_3(t) = \phi(t)$$

Roll angular velocity

$$x_4(t) = \dot{\phi}(t)$$

2) State Equations in Vector Form

Implementing the model easily for control purposes, the simplified state-space model has been presented:

$$\begin{cases} \dot{x}_1(t) = c \cdot x_2(t) \\ \dot{x}_2(t) = -c \cdot x_1(t) + x_4(t) + x_4(t-T) \\ \dot{x}_3(t) = x_4(t) \\ \dot{x}_4(t) = U(t) / I - Cl.q.s.b / I - (b / 2u_\infty I) \cdot \text{sign}(x_4(t)) \cdot x_4(t) \end{cases} \quad (53)$$

3) Vortex Breakdown Locations in New Form

Vortex breakdown locations in new form, without integral term and with state variables are as follows:

$$X_{vbl}(t) = X_{sl} + X_{slkq}(t)x_4(t) + a(t)x_1(t) \quad (54)$$

$$X_{vbr}(t) = X_{sr} + X_{srkq}(t)x_4(t) - a(t)x_1(t) \quad (55)$$

where

$$k_q(t) = 0.91 / \tan(\alpha(t)) \quad (56)$$

III. PARAMETERS AND CALCULATIONS

A. Initial Values for Calculation

The initial values of various system parameters have been calculated using the data reported in [1] as follows:
Structure angle:

$$\sigma_0 = 30 / 57.3 \text{ [rad]} \quad (57)$$

$$\Delta\alpha = 19.8 \cdot \sigma_0 - 5.2 \text{ [deg]} \quad (58)$$

For bevel angle of wing:

$$\sigma = \sigma_0 - (\Delta\alpha / 57.3) \text{ [rad]} \quad (59)$$

Sweep angle:

$$\Lambda_0 = (\pi / 2) - \lambda_0 \text{ [rad]} \quad (60)$$

Release time:

$$T = T^* = 0.1 \text{ [sec]} \quad (61)$$

B. Aerodynamic Parameters and Their Calculations

Free stream velocity:

$$u_\infty = 300 \text{ [ft / sec]} = 91.44 \text{ [m / sec]} \quad (62)$$

Air density:

$$\rho = 1.2 \text{ (kg / m}^3\text{)} \quad (63)$$

Dynamic air pressure:

$$q = 0.5 \rho u_\infty^2 \quad (64)$$

Angle of attack is considered as follows [1]:

$$\alpha(t) = \text{atan}(\cos(\phi) \cdot \tan(\sigma)) \quad (65)$$

Effective sweep back angle:

$$\Lambda_l = \lambda_0 - \text{atan}(\tan(\sigma) \cdot \sin(\phi)) \quad (66)$$

$$\Lambda_r = \lambda_0 + \text{atan}(\tan(\sigma) \cdot \sin(\phi)) \quad (67)$$

Critical circulation:

$$\Gamma_{cl} = 0.8 \cdot \cos[4 \times (\Lambda_l - \Lambda_e)] \quad (68)$$

$$\Gamma_{cr} = 0.8 \cdot \cos[4 \times (\Lambda_r - \Lambda_e)] \quad (69)$$

where,

$$\Lambda_e = 20 \text{ [deg]} \quad (70)$$

is an empirical obtained value.

IV. PARAMETER IDENTIFICATION

Parameter identification is defined as the experimental determination of values of parameters that govern the dynamics and/or nonlinear behaviour, assuming that the structure of the process model is known [19].

Since the control actions on a system depend on the accurate knowledge about the system, in this section, rolling moment coefficient (Cl) as an uncertain parameter in our nonlinear model will be approximated by applying the following methods:

- 1- Linear Least Squares Approximation;
- 2- 3rd order polynomial Approximation;

A. Linear Least Squares Approximation

The rolling moment coefficient is a nonlinear function of vortex breakdown location [1], for now, a linear correlation has been assumed:

$$\Delta X_{vb} = X_{vbl} - X_{vbr} \quad (71)$$

$$Cl(X_{vbl}, X_{vbr}) = e_0 + e_1(\Delta X_{vb}) \quad (72)$$

where X_{vbl} and X_{vbr} represent the breakdown locations for the left and right vortices, e_0 and e_1 are calculated parameters. Fig. 2 shows Cl vs. ΔX_{vb} using linear least square approximation technique.

B. 3rd Order Polynomial Approximation

Third order polynomial curve fitting for Cl approximation as a function of vortex breakdown position, has the following definition:

$$Cl(X_{vbl}, X_{vbr}) = e_0 + e_1(X_{vbl} - X_{vbr}) + e_2(X_{vbl}^2 - X_{vbr}^2) + e_3(X_{vbl}^3 - X_{vbr}^3) \quad (73)$$

where X_{vbl} and X_{vbr} represent the breakdown locations for the left and right vortices, e_0 , e_1 , e_2 and e_3 are calculated parameters. Fig. 6 shows Cl vs. ΔX_{vb} using 3rd order least squares polynomial technique.

V. EXPERIMENTAL VERIFICATION OF NUMERICAL SIMULATION

To verify that the developed nonlinear state space model captures the dynamic behavior of roll mode of the delta wing, we assumed $U(t)=0$ in Eqn (49) and $x1(0) = x2(0) = x4(0) = 0, x3(0) = 58$ [deg] as initial conditions for the numerical simulation. Simulation results are compared to delta wing free-to-roll experimental results obtained from the experimental facility at IAR.

Simulation results for two different rolling moment coefficient (Cl) approximations are shown in Figures 2-9. Fig. 3 and 4 show the open-loop simulation and phase diagram of the plant with linear Cl approximation as the main uncertainty. Fig. 5 shows state variables $x1$ and $x2$ time history obtained with the open-loop simulation and a linear Cl approximation. Fig. 7 and 8 show the open-loop simulation and phase diagram of the plant with a nonlinear Cl approximation. Fig. 9 shows state variables $x1$ and $x2$ time history obtained with open-loop simulations and a nonlinear Cl approximation. It is clear from the figures that the delta wing free-to-roll experimental results validate the proposed nonlinear model of the delta wing. Numerical simulations of the proposed model with 3rd order polynomial approximation of Cl shows superior dynamic behavior when compared with the numerical simulations using the linear Cl approximation, as expected intuitively.

VI. CONCLUSION AND DISCUSSION

The paper proposed a free-to-roll vortex based nonlinear state-space modeling and simulation based on the work done in [1]-[4]. The relationship among the vortex breakdown location, rolling moment coefficient and roll angle were described with four state equations, which constitute a plant model in nonlinear state-space form enabling control synthesis. The proposed model was validated and verified with delta wing free-to-roll experimental results. Two different methods were used for the approximation of the system uncertainty which was rolling moment coefficient ($Cl(X_{vbl}, X_{vbr})$). These methods are linear and nonlinear (3rd order polynomial) curve fitting methods. In the future, better parameter tuning is needed to increase the accuracy of the model, especially correlations for $Cl(X_{vbl}, X_{vbr})$. Neural networks (RBF, wavelet or MLP) can be utilized for this purpose.

ACKNOWLEDGEMENTS

This work was partially funded through the Defence Research and Development Canada (DRDC) Technology Investment Fund under the project entitled 'Supersonic

Missile Flight Control by Manipulation of the Flow Structure using Microactuated Surfaces'. The authors also would like to acknowledge Dr. Huang from NRC-CNRC for his experimental data and helpful scientific support.

REFERENCES

- [1] X. Z. Huang, "Non-Linear Indicial Response and Internal State-Space (NIRISS) Representation and Its Application on Delta Wing Configurations", RTO Technical Report, RTO-TR-047.
- [2] X. Z. Huang, H. Y. Lou, E. S. Hanff, "Non-Linear Indicial Response and Internal State-Space Representation for Free-to-Roll Trajectory Prediction of a 65° Delta Wing at High Incidence", AIAA Paper 2002-4713, 2002.
- [3] X. Z. Huang, Y.Z. Sun, E.S. Hanff, "Circulation Criterion to Predict Leading-Edge Vortex Breakdown Over Delta Wings", AIAA Paper 1997-2265, 1997.
- [4] X. Z. Huang, E. S. Hanff, "Prediction of Normal Force on a Delta Wing Rolling at High Incidence", AIAA paper 93-3686, Aug. 1993.
- [5] P. H. Reisenel, "Development of a Nonlinear Indicial Model for Maneuvering Fighter Aircraft", AIAA 96-0896, 1996.
- [6] P. H. Reisenel, "Application of Nonlinear Indicial Modeling to the Prediction of a Dynamically Stalling Wing", AIAA 96-2493, 1996.
- [7] P. H. Reisenel, "Development of a Nonlinear Indicial Model Using Response Functions Generated by a Neural Network", AIAA 97-0337, 1997.
- [8] P. H. Reisenel, M. T. Bettencourt, "A Nonlinear Indicial Prediction Tool for Unsteady Aerodynamic Modeling", AIAA 98-4350, 1998.
- [9] P. H. Reisenel, W. Xie, I. Gursul, M. T. Bettencourt, "An Analysis of Fin Motion Induced Vortex Breakdown", AIAA 99-0136, 1999.
- [10] P. H. Reisenel, M. T. Bettencourt, "Data-Based Aerodynamic Modeling Using Nonlinear Indicial Theory", AIAA 99-0763, 1999.
- [11] P. H. Reisenel, M. T. Bettencourt, "Extraction of Nonlinear Indicial and Critical State Response from Experimental Data", AIAA 99-0764, 1999.
- [12] B. N. Pamadi, P. C. Murphy, V. Klein, Jay M. Brandon, "Prediction of Unsteady Aerodynamic Coefficients at High Angles of Attack", NASA Center for AeroSpace Information (CASI), AIAA Paper 2001-4077, Aug. 2001.
- [13] P. H. Reisenel, "Prediction of Unsteady Aerodynamic Forces via Nonlinear Kernel Identification", CEAS / AIAA / ICASE / NASA Langley International Forum on Aeroelasticity and Structural Dynamics, Williamsburg, VA, June 22-25, 1999.
- [14] M. Goman, A. Khrabrov, "State-Space Representation of Aerodynamic Characteristics at High Angles of Attack", Journal of Aircraft, Vol. 31, No. 5, pp. 1109-1115, Sept.-Oct. 1994.
- [15] V. Klein, K. D. Noderer, "Modeling of Aircraft Unsteady Aerodynamic Characteristics, Part 1 - Postulated Models", NASA Technical Memorandum 109120, May 1994.
- [16] M. Tobak, G. T. Chapman, L. B. Schiff, "Mathematical Modeling of the Aerodynamic Characteristics in Flight Dynamics", NASA-TM-85880, 1984.
- [17] M. Tobak, L. B. Schiff, "Aerodynamic Mathematical Modeling - Basic Concepts", NASA Center for AeroSpace Information (CASI), 1981.
- [18] L. B. Schiff, M. Tobak, G. N. Malcolm, "Mathematical Modeling of the Aerodynamics of High-Angle-of-Attack Maneuvers", AIAA Paper 80-1583, Atmospheric Flight Mechanics Conference, Danvers, MA, Aug. 1980.
- [19] Pieter Eykhoff, "System Identification, Parameter and State Estimation", John Wiley & Sons Ltd., 1974.

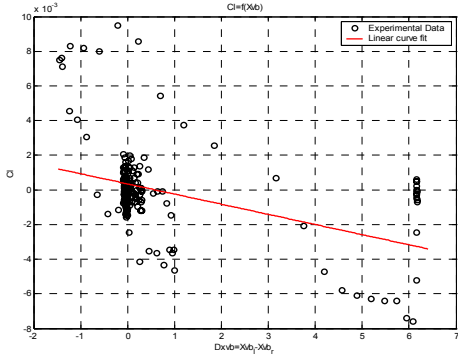


Fig. 2. Cl linear approximation

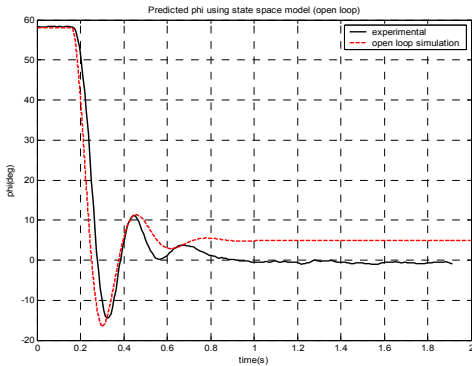


Fig. 3. Open loop simulation using Cl linear approximation

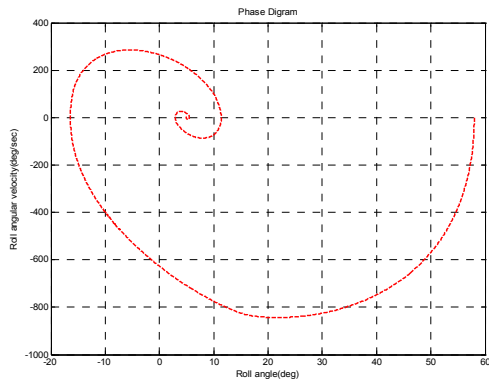


Fig. 4. Phase diagram for the system with Cl linear approximation

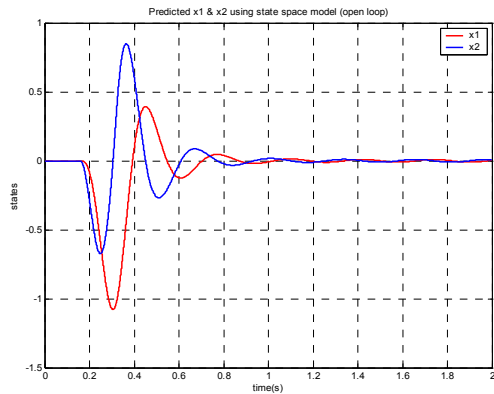


Fig. 5. x_1 and x_2 state variables history with Cl linear approximation

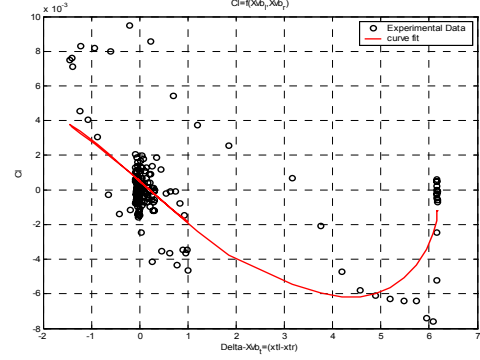


Fig. 6. Cl nonlinear approximation

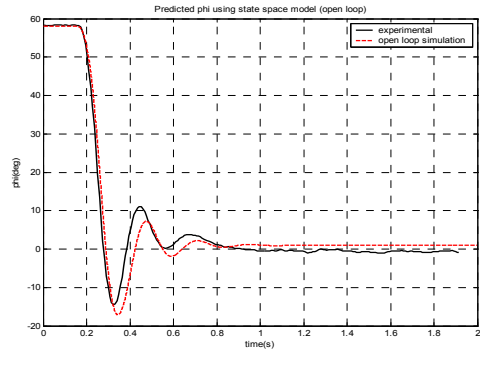


Fig. 7. Open loop simulation using Cl nonlinear approximation

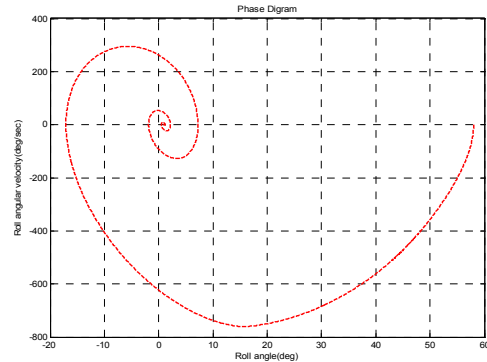


Fig. 8. Phase diagram for the system with Cl nonlinear approximation

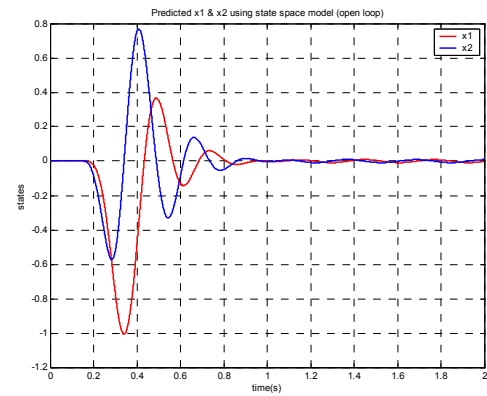


Fig. 9. x_1 and x_2 state variables history with Cl nonlinear approximation